



Novel biomarker profiles in experimental aged maternal mice with hypertensive disorders of pregnancy

Kiichiro Furuya¹ · Keiichi Kumasawa¹ · Hitomi Nakamura¹ · Katsuhiko Nishimori² · Tadashi Kimura¹

Received: 16 August 2017 / Revised: 26 February 2018 / Accepted: 14 March 2018 / Published online: 13 September 2018
© The Japanese Society of Hypertension 2018

Abstract

Recently, advanced maternal age (AMA) has increased in Western countries because of late marriage and advances in assisted reproductive technology. One major complication of AMA is hypertensive disorders of pregnancy (HDP). While clinical investigations into human AMA have been reported, there has been limited information obtained from basic research. In this investigation, we established the AMA mouse model using aged pregnant ICR mice. We demonstrated that the phenotypes of aged pregnant ICR mice reflect the same characteristics as human AMA. The significant findings of our investigation are as follows: (1) The AMA mouse model manifested the same complication phenotypes of human AMA, including maternal obesity, declining fertility, small for gestational age, and a higher rate of intrauterine fetal death; (2) The AMA mouse model exhibited an increasing systolic blood pressure at late gestation (108.2 ± 7.7 vs. 92.7 ± 5.7 mmHg, $P < 0.01$) that normalized after delivery similar to human HDP patients; and (3) While HDP and placental dysfunction are complicated, AMA mice and human HDP AMA patients manifested a low serum soluble fms-like tyrosine kinase-1 (sFlt-1) level in late gestation (AMA group vs. control group, mice, 16800.0 ± 10709.5 vs. 26611.9 ± 8702.0 pg/mL, respectively, $P < 0.01$; human, 8507.6 ± 3298.7 vs. 14816.9 ± 5413.5 pg/mL, respectively, $P < 0.05$). In conclusion, the aged pregnant mouse model resembled human AMA. The AMA mouse model was complicated with HDP despite the low serum sFlt-1 level. Our findings provide evidence that the serum sFlt-1 level does not necessarily reflect the conventional pathogenesis of HDP in aged human and murine pregnancies and may contribute to the future management of HDP in AMA.

Introduction

Recently, advanced maternal age (AMA) pregnancy have been increasing in Western countries because of late marriage and advances in assisted reproductive technology (ART) [1–4]. AMA is associated with maternal and fetal mortality and morbidity [2, 5–7]. In particular, hypertensive

disorders of pregnancy (HDP) is one of the major complications in AMA [1, 2]. While clinical research on human AMA has been reported, there has been limited information from basic research using mouse models suitable for AMA research. Furthermore, the mechanisms of HDP complicated with AMA remain unclear. Several HDP animal models have previously been reported; however, they were artificially established using surgical and transgenic approaches [8–11]. These animal models have been insufficient to investigate the relationship between the likeliness of the onset of HDP and late pregnancy. We examined the effects of blood pressure and analyzed whether HDP spontaneously develops using aged pregnant mice. The purposes of this study were to establish an AMA mouse model, compare its phenotypes to human AMA, and verify the pathogenesis of HDP in AMA. The noteworthy points included the complicated phenotypes associated with AMA and HDP patients, blood pressure (BP), and the key factors of HDP: serum soluble fms-like tyrosine kinase-1 (sFlt-1) and placental growth factor (PlGF).

Electronic supplementary material The online version of this article (<https://doi.org/10.1038/s41440-018-0092-7>) contains supplementary material, which is available to authorized users.

✉ Keiichi Kumasawa
kumasawa@gyne.med.osaka-u.ac.jp
kokoko52@hotmail.com

¹ Department of Obstetrics and Gynecology, Osaka University Graduate School of Medicine, Osaka, Japan

² Department of Molecular and Cell Biology, Graduate School of Agricultural Science, Tohoku University, Tohoku, Japan

Materials and methods

Animals

Refer to supplementary information.

Aged and young mice

The AMA mouse model was defined as pregnant Jcl:ICR female mice more than 6 months old. Control Jcl:ICR female mice were defined as 8–13 weeks old at pregnancy. Refer to supplementary information for the details.

Blood pressure measurement

Blood pressure measurement was performed as previously reported [8].

Anesthesia

Refer to supplementary information.

Fetal weight and litter size measurement (mouse model)

For evaluation of the clinical complications of human AMA at term, we analyzed the following factors: fertility decline, small for gestational age (SGA), and intrauterine fetal death (IUFD) rates. All fetuses and placentas were removed by cesarean section at E18.5 (i.e., term pregnancy in mice). The samples were weighed and numbered. The experimental procedures described are as follows. The mice received sevoflurane anesthesia, were held on a hot plate, and were subjected to abdominal sterilization, followed by vertical incision of the abdominal wall. The uterus was exteriorized from the incision, and the pups were removed from the uterus by cesarean section [8, 12]. The percentage of IUFD was defined as the number of IUFD for all pups (%).

Blood and urinary samples

Serum samples from mice were collected as described in our previous report [8]. Serum samples from HDP patients at 36–38 weeks of gestation were obtained from Osaka University Medical Hospital (Ethics committee registration no. 17381). The serum levels of sFlt-1 and PlGF-2 in mice and sFlt-1 and PlGF in humans were measured with ELISA kits (R&D Systems, USA). Urinary protein levels were analyzed with VetScan VS2 (Abaxis, USA).

Tissue collection (Snap freezing and RNA extraction)

Tissue collection and RNA extraction were performed as previously described [8, 13].

Real time PCR (RT-PCR)

Following DNase treatment (TURBO DNA-free Kit, Thermo Fisher Scientific, USA), 2 µg of total RNA was reverse transcribed into complementary DNA (cDNA) using SuperScript VILO Mastermix (including SuperScript III reverse transcriptase, Invitrogen, USA) according to the manufacturer's protocol. Real time PCR (RT-PCR) was performed using SYBR-Green (Applied Biosystems, USA). We used primer sets to amplify mouse *p53* and mouse *hif1-α*, which have been used in previous reports. The primers for mouse *p53* were: 5'-CCCGAGTATCTGGAAGACAG-3' (forward) and 5'-ATAGGTGGCGGTTTCAT-3' (reverse) [14–16]. The primers for mouse *hif1-α* were: 5'-CAAGATCTCGGCGAAGCAA-3' (forward) and 5'-GGTGAGCCTCATAACA-GAAGCTTT-3' (reverse) [17]. We also used a primer set for human *sflt-1*. The primers for human *sflt-1* were: 5'-ACA ATC AGA GGT GAG CAC TGC AA-3' (forward) and 5'-TCC GAG CCT GAA AGT TAG CAA-3' (reverse).

Perfusion fixation

Perfusion fixation was performed using 4% paraformaldehyde (PFA). Refer to the supplementary information for further details.

Tissue processing

Paraffin-embedded sections: After perfusion fixation, tissue samples were immersed in 4% PFA for 36 h at 4 °C, rinsed with flowing water for 1 h, dehydrated and permeated with ethanol and xylene, and embedded in paraffin. The blocked tissue was sectioned at 3–4 µm (SM2000R, Leica), dried, and placed on a heat pad overnight.

Cell culture

The human trophoblast-derived cell line HTR-8/SVneo, purchased from the manufacturers (American Type Culture Collection; ATCC, USA), was cultured at 37 °C in a 5% CO₂ incubator in RPMI 1640 medium that contained 5% fetal bovine serum (FBS) in a 6 well cell culture plate (FALCON, USA).

Table 1 Characteristics of AMA model mice and control mice before and during pregnancy

| | Control (n) | Aged (n) | P value |
|--|-----------------|-----------------|-----------------|
| Age (weeks) | 13.7 ± 2.3 (26) | 33.0 ± 9.7 (28) | <i>P</i> < 0.05 |
| Before pregnancy BW (g) | 32.1 ± 3.5 (16) | 47.1 ± 9.4 (24) | <i>P</i> < 0.05 |
| E18.5 BW (g) | 72.1 ± 5.3 (16) | 73.5 ± 9.3 (24) | <i>P</i> = 0.60 |
| Pregnancy BW gain (From before pregnancy to E18.5) (g) | 40.1 ± 4.3 (16) | 26.9 ± 9.2 (24) | <i>P</i> < 0.05 |
| BW gain per fetus (g) | 2.9 ± 0.5 (15) | 2.4 ± 0.5 (20) | <i>P</i> < 0.05 |
| Rate of IUFD (%) ^a | 1.1 ± 2.8 (23) | 9.9 ± 17.8 (30) | <i>P</i> < 0.05 |

Data are presented as the mean ± SD. All numbers of aged and control pregnant mice are shown in parentheses

BW body weight, E embryonic day, IUFD intrauterine fetal death

^aRate of IUFD: (number of fetal deaths/number of fetuses) multiplied by 100 (%). Student's *t*-test was performed against control mice

H₂O₂ treatment and sample collection

Eighty to ninety percent confluent HTR-8/SVneo cells were exposed to a range of H₂O₂ concentrations from 0 to 200 μM for 2 h. This treatment has been reported to induce artificial senescence conditions according to several reports [18–21]. All cells and cell cultures were collected after H₂O₂ treatment. RNA and proteins were extracted from the collected cells after treatment.

Senescence-associated beta-galactosidase (SA-β-gal) staining

Staining of SA-β-gal, which is a senescence marker [20, 22], was performed according to the manufacturer's instructions (Abcam, USA). Stained cells were observed microscopically by using one hundred-fold magnification (BZ-X700, KEYENCE, Japan). The positive staining dots for SA-β-gal were quantified (*n* = 6 fields per dish under one hundred-fold magnification; three wells per concentration group).

NO determination

NO is stoichiometrically converted to nitrate (NO₃⁻) and nitrite (NO₂⁻), the stable metabolites of NO. Therefore, the NO levels were determined by measuring NO₃⁻ and NO₂⁻. The NO levels in the cell culture supernatants were measured as the total NO₂⁻ (NO₂⁻ and NO₂⁻ converted from NO₃⁻) by using a Nitric Oxide Colorimetric Assay Kit (BioVision, USA).

Statistics

All data are presented as the mean and standard deviation (mean ± SD), and nonparametric statistical analysis was applied for the limited numbers in the experiments. The differences between multiple groups were analyzed by a one-way or two-way analysis of variance (ANOVA) with

Tukey's post-hoc test. Student's *t*-test was used for comparisons between the two groups. *P* values of < 0.05 indicated significant differences.

Results

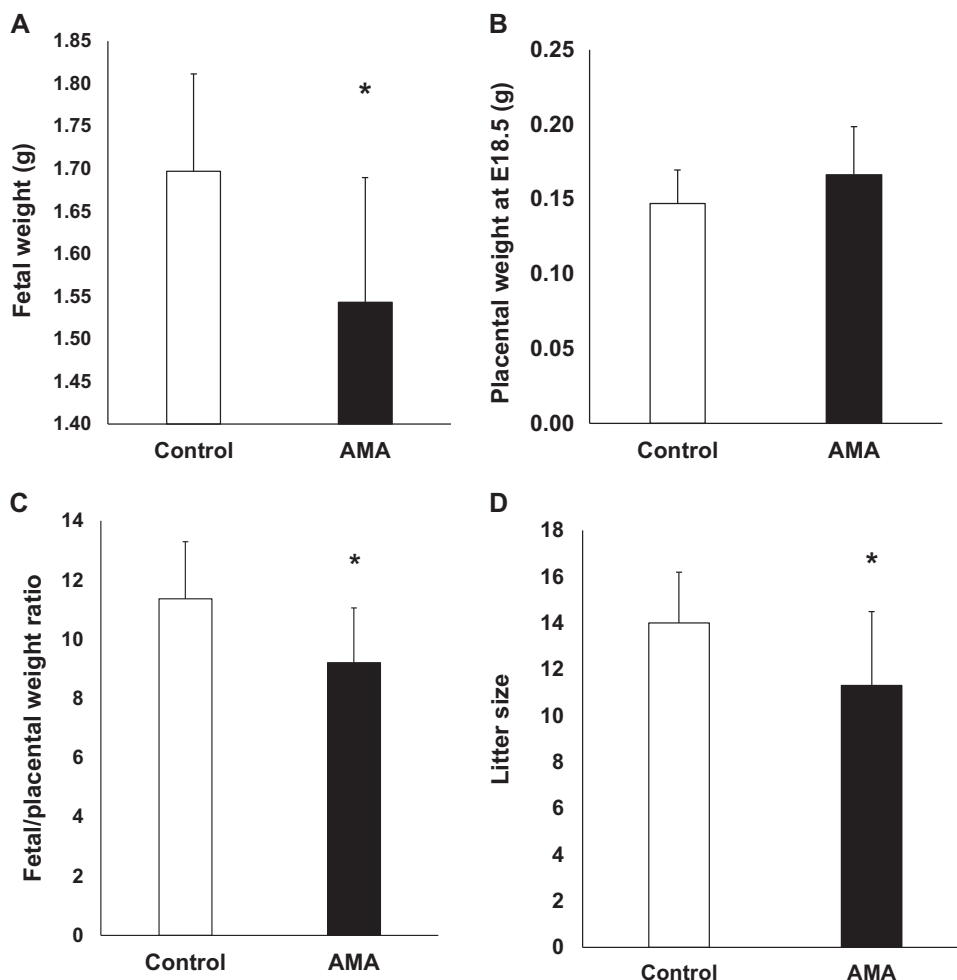
Characterization of the AMA mouse model

The characteristics before and after pregnancy in both groups are shown in Table 1. The age and body weight before pregnancy manifested a wide range in both groups. The maternal body weight before pregnancy in the AMA mice was significantly heavier than in the control mice. The body weights of the AMA mice at E18.5 were not significantly heavier than those of the control mice. The visceral fatty tissues before pregnancy, at E14.5, and at E18.5 were not significantly different in both groups. The weight of brown fat tissue was not significantly different between the AMA mice and young mice, as a result of individual differences (Supplementary Figure 3). The fetal weight for the AMA mice was significantly decreased compared with that of the control mice (Fig. 1a). The placental weight was not significantly different between the two groups (Fig. 1b). In contrast, the fetal/placental weight ratio in the AMA mice was significantly smaller than in the control mice (Fig. 1c). The litter size of the AMA mice was significantly less than that of the control mice (Fig. 1d). The IUFD rates of the AMA mice were significantly higher than those of the control mice (Table 1).

Evaluations of phenotypes of HDP in the AMA mouse model

Blood pressure was measured before pregnancy, at E8.5, at E18.5, and postdelivery within one week in both groups. The systolic blood pressure before pregnancy was not significantly different in both groups, whereas the systolic blood pressure of the AMA mice at E18.5 was significantly

Fig. 1 Pregnancy outcomes in AMA and control mice: **a** Fetal weight (AMA; $n = 11$, Control; $n = 12$), **b** placental weight at E18.5 (AMA; $n = 11$, Control; $n = 12$), **c** fetal/placental weight ratio (AMA; $n = 11$, Control; $n = 12$), and **d** Litter size (AMA; $n = 30$, Control; $n = 23$). Data are presented as the mean \pm SD. * $P < 0.05$ vs. control mice



higher than that of the control mice. After delivery, the blood pressure of the AMA mice recovered to the same level as that of the control mice (Fig. 2a). The protein/creatinine ratio of urine was not significantly different between the AMA and control mice throughout pregnancy (Fig. 2b).

Angiogenic factors of HDP in the AMA mouse model and human AMA

The serum level of mouse sFlt-1 increased with pregnancy in both groups. The AMA mice had increasing blood pressure at late gestation, whereas the serum sFlt-1 levels were significantly lower than those in the control mice at E18.5 + E19.5 before delivery (AMA mice: 16800.0 ± 10709.5 vs. control mice: 26611.9 ± 8702.0 pg/mL, $P < 0.05$, Fig. 3a). The serum PIGF-2 in the AMA mice at late gestation was also significantly lower than in the control mice (Fig. 3b). Human serum sFlt-1 and serum PIGF were measured using serum samples obtained from “aged” (over 40 years old) and “young” (under 30 years old) HDP

patients who delivered at Osaka University Medical Hospital. Similar to the mouse results, the serum sFlt-1 level in the aged HDP patients was significantly lower than that of the young HDP patients (Aged HDP patients: 7174.9 ± 3698.9 vs. young HDP patients: 14816.9 ± 5413.6 pg/mL, $P < 0.05$, Fig. 3c).

To evaluate the biomarker profiles between blood pressure and vessel or tissue aging at the gene transcription level in the AMA model mice, an investigation was performed using real-time PCR (RT-PCR). The expression of *p53* in the fatty and placental tissues of the AMA mice at E18.5 was significantly higher than in those of the control mice (Fig. 4a, b). The expression of *hif1- α* in the placenta of the AMA mice was also significantly elevated at E18.5 compared with that of the control mice (Fig. 4c). In immunohistopathological staining of the uterine artery, positive p53 staining in the AMA mice increased during the course of gestation to reach its highest level at E18.5; however, the level of p53 staining was very low in the control mice at the same period (Supplementary Figure 6).

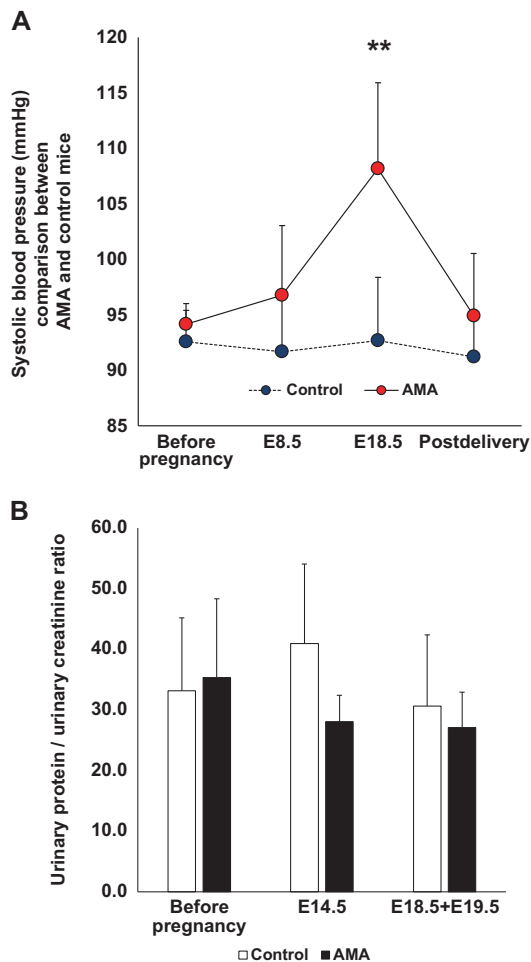


Fig. 2 **a** Systolic blood pressure was measured before pregnancy, E8.5, E18.5, and postdelivery, comparing AMA (Before pregnancy; $n = 10$, E8.5; $n = 10$, E18.5; $n = 11$, and postdelivery; $n = 6$) and control mice (Before pregnancy; $n = 8$, E8.5; $n = 6$, E18.5; $n = 15$, and postdelivery; $n = 7$). $**P < 0.01$ vs. control mice. Data are presented as the mean \pm SD. **b** Urinary protein/urinary creatinine ratio was measured before pregnancy (AMA; $n = 4$, Control; $n = 5$), E14.5 (AMA; $n = 3$, Control; $n = 4$), and E18.5 + E19.5 (before delivery: AMA; $n = 7$, Control; $n = 8$), and AMA and control mice were compared. Data are presented as the mean \pm SD

Induction of senescence conditions in HTR-8/SVneo cell line

The SA- β -gal staining intensity significantly increased in a dose-dependent manner for $H_2O_2^-$ treated HTR-8/SVneo cells (Fig. 5a, b).

Senescent cells showed low sFlt-1 and NO_2^- levels

The levels of NO_2^- significantly decreased in a dose-dependent manner for $H_2O_2^-$ treated HTR-8/SVneo cells (Fig. 5c). In RT-PCR, the expression of *sflt-1* in HTR-8/SVneo increased in a dose-dependent manner from 0 to 150 μM H_2O_2 supplementation; however, the expression of

sflt-1 in cells treated with 200 μM H_2O_2 was significantly decreased (Fig. 5d).

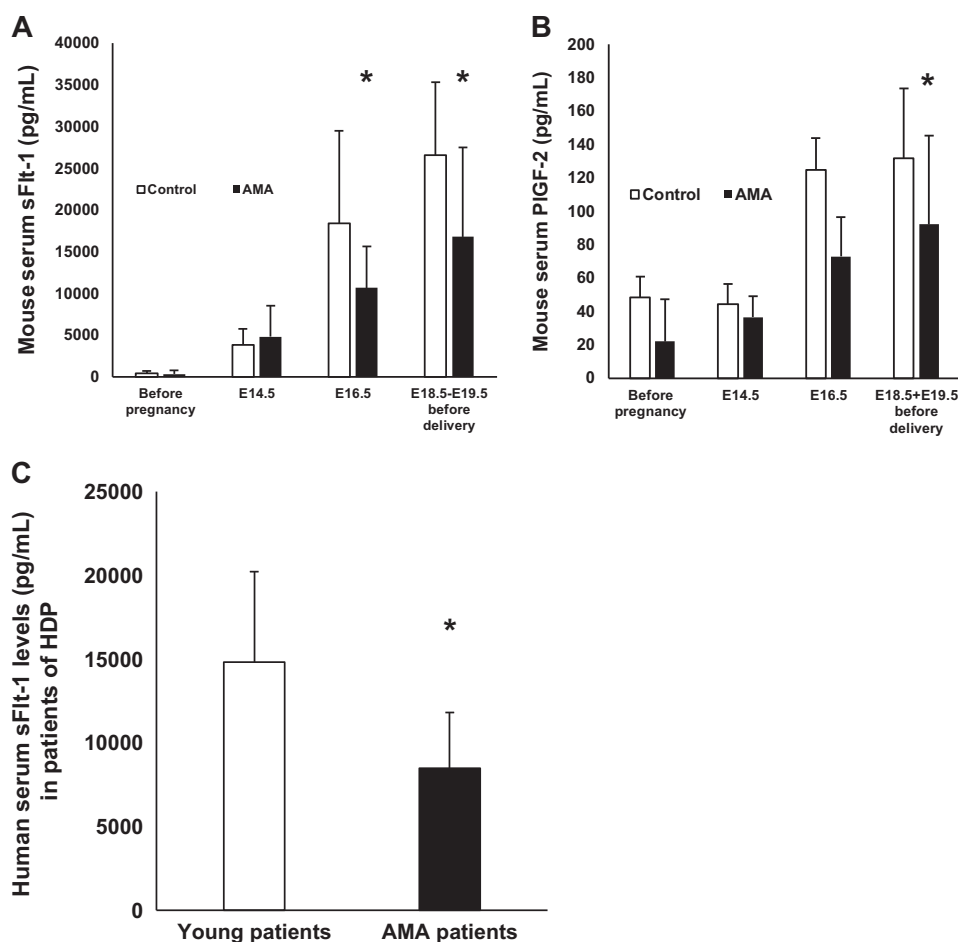
Discussion

AMA is associated with many complications, with HDP representing one of the major perinatal problems for mothers and babies. Moreover, epidemiological investigations have recently indicated that a history of HDP is associated with the future risk of heart disease, stroke, arrhythmia, diabetes mellitus, renal failure, and hypertension [23]. Therefore, various methods have been used in experiments to predict HDP. For example, the sFlt-1/PlGF ratio [24] and serum angiotensin-2 levels have been assessed with uterine artery Doppler [25]. In this investigation, we established the AMA mouse model and evaluated its complication phenotypes to assess the contributing factors between middle-age pregnancy and hypertensive disorder in pregnancy. First, we demonstrated that the aged pregnant ICR mouse manifested the same characteristics of human AMA without genetic or mechanical interventions. Second, the AMA mouse model had an increasing systolic blood pressure in the late gestation period, thus reflecting human HDP. Third, while the AMA mouse model demonstrated hypertension and a low serum PlGF level, which reflects placental dysfunction, the serum sFlt-1 level in the AMA mice was significantly lower than that in the control mice. This phenomenon was also identified for the serum sFlt-1 profile in human AMA complicated with HDP. To the best of our knowledge, these results are the first evidence of low serum sFlt-1 levels in AMA mice and human AMA HDP patients. These results showed that the AMA mouse model had the same features as human AMA, which should make it useful for in vivo studies of human AMA. In AMA complicated with HDP, it may be necessary to establish a new standard value for serum sFlt-1 levels.

AMA mouse model had the same complications of human AMA

Human AMA is associated with maternal and fetal mortality and morbidity. The fetal risks in human AMA include increased miscarriage, aneuploidy, IUGR, and IUFD [2, 5–7]. AMA also involves maternal complications, such as HDP, which is one of the most life-threatening complications [2, 26]. We verified whether our mouse model had the same major complications, such as hypertension, as human AMA. In our mouse model, aged pregnant ICR mice represented a wide range of ages and body weights (Table 1). These results reflected the physical conditions of human AMA consisting of women ranging from 35 to approximately 40 years of age. IUGR and IUFD were

Fig. 3 sFlt-1 (a) and PIGF-2 (b) in AMA (sFlt-1; $n = 5-16$, PIGF; $n = 5-16$) and control mice (sFlt-1; $n = 5-12$, PIGF; $n = 5-12$). Data are presented as the mean \pm SD. * $P < 0.05$ vs. control mice. **c** Human sFlt-1 in patients with HDP comparing patients over 40 years old ($n = 7$) and patients under 30 years old ($n = 5$). Data are shown in a vertical column chart and presented as the mean \pm SD. * $P < 0.05$ vs. patients under 30 years old



significantly increased in the AMA mouse model (Fig. 1a; Table 1). It is well known that age-related aneuploidy chromosomes in murine oocytes are very rare [27]. Therefore, we did not verify the existence of chromosomal abnormalities in our mouse model.

AMA mouse model represented HDP as well as human AMA

In our mouse model, proteinuria was not observed in both groups, whereas systolic blood pressure in the AMA mouse model at late gestation was 15.5 mmHg (16.2%), which is higher than in control mice at the same time ($P = 0.01$). The systolic blood pressure of both groups was at the same level before and during early pregnancy. These results corresponded with a previous report indicating that over 50% of human AMA is complicated by hypertensive disorder [2]. It is important to distinguish between HDP and essential hypertension. In this study, blood pressure decreased within weeks after delivery. Therefore, the AMA model mice turned out not to be essential hypertension but was HDP. According to the current criteria, in some cases, HDP is discussed without the complication of proteinuria [28–30].

From our results and recent criteria, the AMA mouse model was complicated with HDP at term pregnancy similar to human AMA. The serum PIGF-2, an angiogenesis factor that reflects placental function, was significantly decreased in the AMA mouse model during late gestation. Moreover, the expression of hypoxia induced factor 1- α (HIF1- α) of AMA at E18.5 was significantly higher than that of control mice (Fig. 4c). These results also indicated and supported the existence of placental dysfunction as the pathogenesis of HDP. These results demonstrated that increasing blood pressure in the AMA mouse model at late gestation could be defined as HDP, including gestational hypertension (GH). In our results, AMA model mice represented the characteristics of gestational hypertension as the subtypes of the new criteria of HDP. Additionally, the AMA mouse model had similarities to the life-threatening maternal complications present in human AMA.

Profiles of biomarkers associated with HDP in AMA

According to the current investigations, the “two step theory” has been advocated as the pathogenesis of HDP. Placental dysfunction is associated with the development of

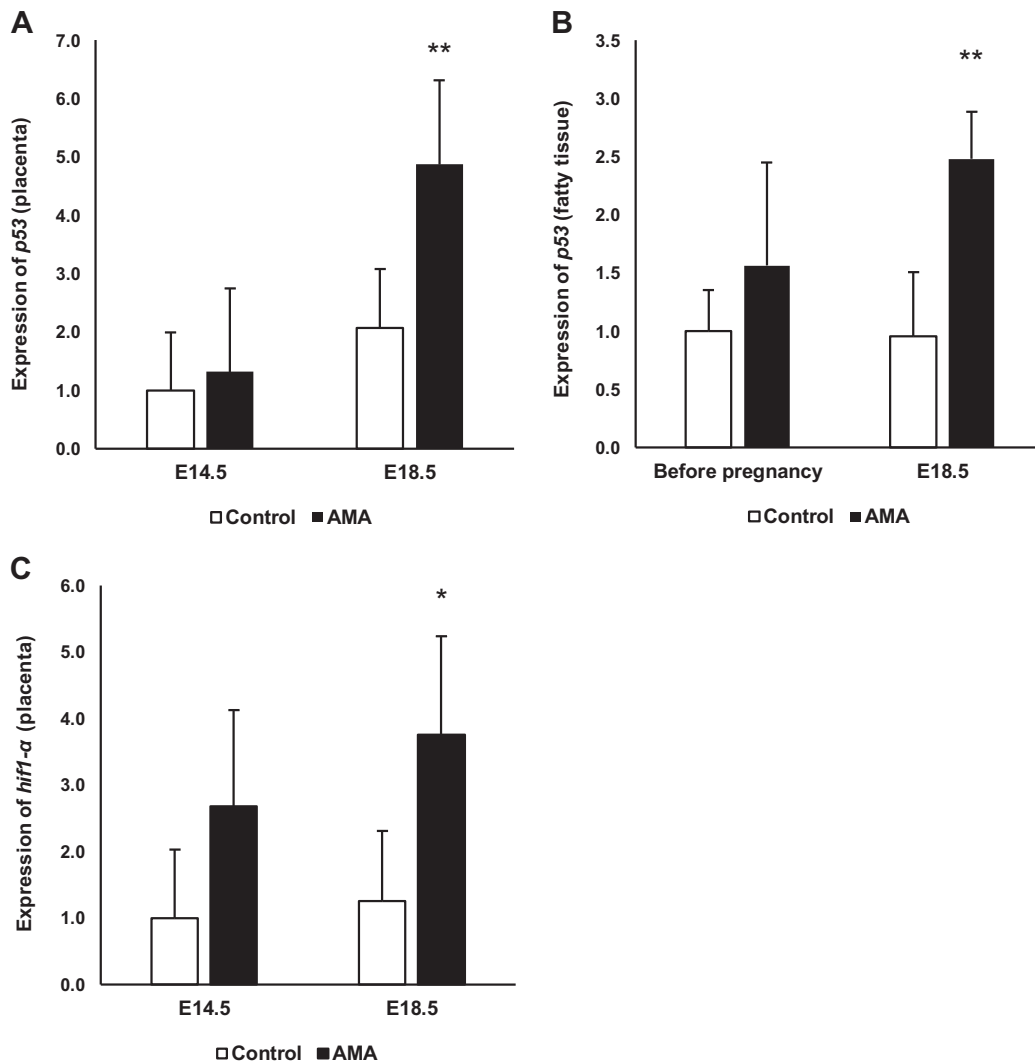


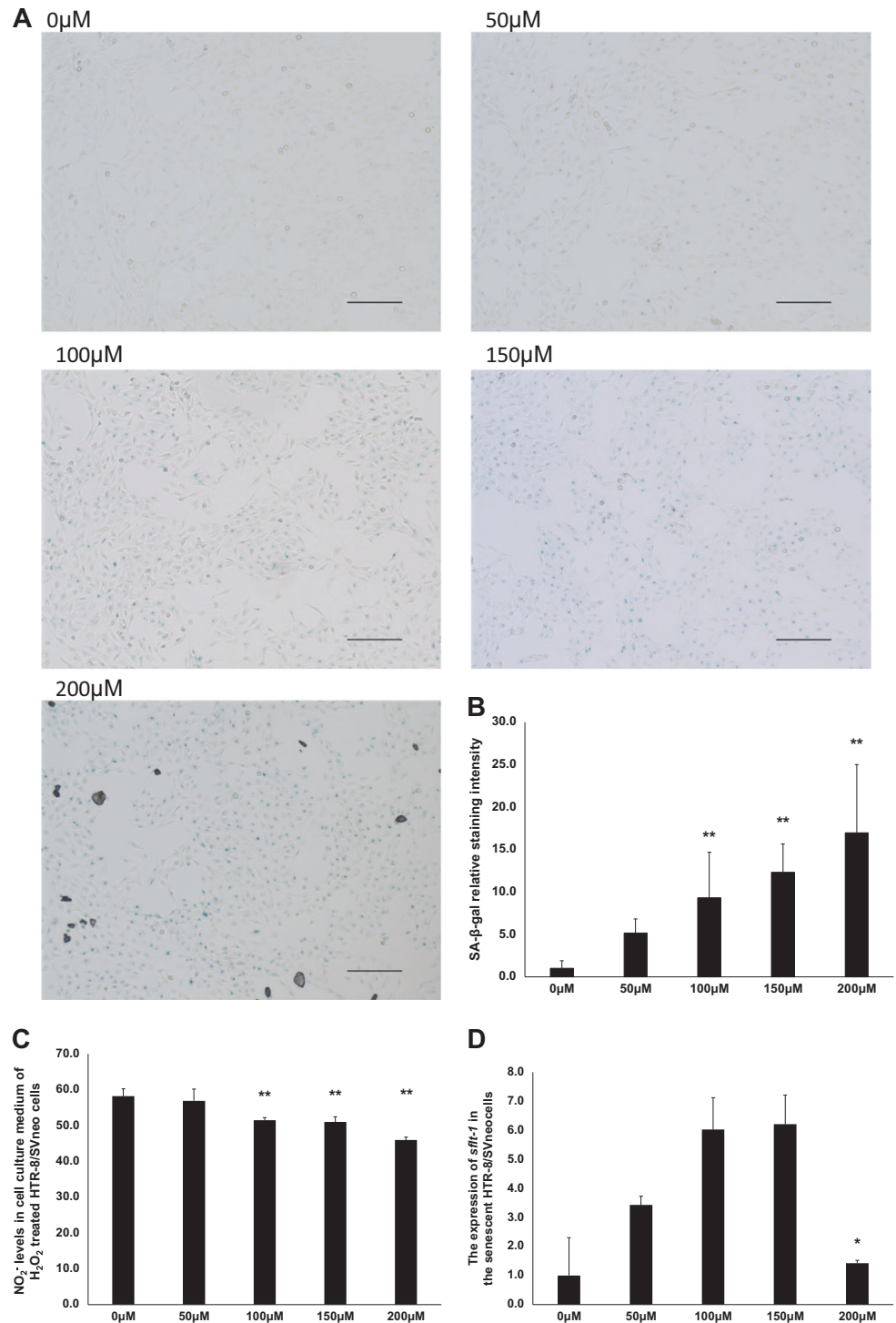
Fig. 4 **a** Expression of *p53* in placenta (E14.5 vs. E18.5, AMA; $n = 4$, control; $n = 3$) and **b** fatty tissue (before pregnancy vs E18.5, AMA; $n = 2$, control; $n = 3$) in AMA and control mice. **c** *hif1- α* gene expression in the placenta comparing AMA and control mice at E14.5

(AMA vs. control; $n = 4$ vs. $n = 3$) and E18.5 (AMA vs. control; $n = 3$ vs. $n = 2$). The black bar represents the AMA group, and the white represents the control group. The results are presented as the mean \pm SD. * $P < 0.05$ vs. control mice. ** $P < 0.01$ vs. control mice

hypertension during pregnancy [9, 31–33]. In current clinical investigations, the anti-angiogenic factor soluble fms-like tyrosine kinase-1 (sFlt-1), which antagonizes vascular endothelial growth factor, has been reported as the key factor for human HDP. The angiogenic factor placental growth factor (PlGF) is decreased in HDP. Clinical studies have reported that increased serum sFlt-1 level and decreased serum PlGF level correspond to the severity of HDP; [34–37] however, investigation into these factors in AMA patients is insufficient. Surprisingly, blood pressure in the AMA mouse model at E18.5 + E19.5 was increased, whereas the serum sFlt-1, the critical factor of HDP, was significantly lower than in the control mice ($16,800.0 \pm 10,709.5$ ($n = 16$) vs. $26,611.9 \pm 8,702.0$ ($n = 12$) pg/mL, respectively, $P < 0.05$; Fig. 3a). These data are the first evidence that the serum sFlt-1 in aged pregnant mice

complicated with HDP exhibited low levels despite being complicated by HDP. In previous studies in humans, the age groups of “aged” HDP patients from whom serum samples were obtained for HDP investigations have been approximately 35–40 years old [38, 39]. To the best of our knowledge, no previous reports have analyzed these factors using subjects who were of extremely AMA (over 40 years old) with HDP. Therefore, we measured human serum sFlt-1 obtained from HDP patients, including individuals who were of extremely AMA over 40 years of age. Surprisingly, the human serum sFlt-1 levels in extremely AMA patients were significantly lower than those of the young patients (7174.9 ± 3698.9 pg/mL; extremely AMA patients ($n = 8$) vs. $14,816.9 \pm 5413.6$ pg/mL; young patients ($n = 5$), $P < 0.05$; Fig. 3c), which is consistent with the results in our mouse model. The mechanism of this effect

Fig. 5 H₂O₂ supplementation in HTR-8/SVneo cells induced senescence. **a** SA-β-gal staining increased in high H₂O₂ concentration-treated HTR-8/SVneo cells. Blue dots show positive SA-β-gal staining. Scale bar: 200 μm **b** SA-β-gal relative staining intensity in H₂O₂-treated HTR-8/SVneo cells; the positive staining for SA-β-gal was quantified ($n = 6$ fields per well under x100 magnification; three wells per H₂O₂ concentration group). **c** NO₂⁻ level in cell culture medium of H₂O₂-treated HTR-8/SVneo cells ($n = 3$ per H₂O₂ concentration group). **d** The expression of *sflt-1* in senescent HTR-8/SVneo cells decreased in an H₂O₂ dose-dependent manner ($n = 3$ per H₂O₂ concentration group). The results are presented as the mean ± SD. * $P < 0.05$ vs. 0 μM group. ** $P < 0.01$ vs. 0 μM group



remains unclear; however, we demonstrated that the experimental results in vivo corresponded with the clinical results.

While the aged pregnant mice and AMA were complicated with HDP, serum sFlt-1 demonstrated a low level. To verify the cause of hypertension in AMA, we focused on the

vessel senescence and arteriosclerosis as a result of the expression of p53, which is a well-known aging marker and a key signal of senescence [40–42]. Previous researchers have reported that arteriosclerosis and endothelial dysfunction result in hypertension. They cause hypertension and are one of the processes of aging [43–45]. Therefore, it

was important to examine p53 expression in vessels and tissues. Investigations have reported that blood vessel senescence plays a role in the development of hypertension. The aged cell accelerates arteriosclerosis because of the secretion of inflammatory cytokines. Endothelial cells with a high expression of p53 and high activation of SA- β -gal are observed on the plaques present in human coronary arteriosclerosis [43–46]. The development of arteriosclerosis and vessel injury as a result of metabolic disease is also associated with vessel cell senescence involved in the activation of p53. It has been demonstrated that the endothelial cell senescence triggered by p53 signal activation plays an important role in promoting arteriosclerosis and decreasing angiogenesis by hypertension and diabetes [46, 47]. Therefore, it has been demonstrated that metabolic and age-related factors stimulate blood vessel senescence and progress hypertension. These results indicate that arteriosclerosis and hypertension are associated with vessel senescence.

In our AMA mouse model, the expression of *p53* in the placenta and fatty tissues was significantly higher than that in control mice (Fig. 4a, b). The placental dysfunction in the AMA mouse model was implied by the increasing expression of *p53* in the placenta and the low serum PIGF-2 levels late in gestation. These results support the finding that the AMA mouse model involves factors associated with HDP and indicate that AMA could result in HDP with low serum sFlt-1. This investigation of our AMA mouse model shows the progression of vessel and tissue senescence during the course of pregnancy. These tissue senescence observations may contribute to hypertension in the AMA mouse model. These results show that the AMA mouse model has the same features of complications, such as hypertension, in advanced-age pregnancies in women despite low serum sFlt-1 levels.

H₂O₂⁻supplemented HTR-8/SVneo cells showed senescence conditions

We subsequently investigated cell senescence in the human trophoblast cell line HTR-8/SVneo to elucidate the mechanisms by which blood pressure increased with lower sFlt-1 levels in aged HDP patients and the AMA mouse model. One of the best-known ways to induce senescence in cells is H₂O₂ supplementation [19, 20]. We attempted to induce senescence in the human trophoblast cell line HTR-8/SVneo as described in previous reports [18, 21]. As previously reported, several concentrations of H₂O₂ (0–200 μ M) were supplemented in HTR-8/SVneo cell culture medium [18, 21, 48, 49]. H₂O₂⁻ supplemented cells exhibited a high intensity of SA- β -gal staining in a dose-dependent manner. This result indicates that the cell senescence advanced depending on the H₂O₂ concentrations.

Artificial senescence-induced human trophoblast cells showed low NO₂⁻ levels and low expression of *sflt-1*

Both aged HDP patients and AMA model mice represented phenotypes of HDP; moreover, the serum sFlt-1 levels were significantly lower than those in control groups. To understand the characteristics of aged HDP patients and the AMA mouse model, we elucidated the expression of *sflt-1* and NO₂⁻ levels using the HTR-8/SVneo cell line and cell culture medium that contained H₂O₂. The expression of *sflt-1* increased with concentrations of H₂O₂ from 50 to 150 μ M; however, it significantly decreased at 200 μ M. This result was consistent with the low level of sFlt-1 in human AMA-HDP patients and the AMA mouse model.

We subsequently measured NO₂⁻, which is an established vasodilator. From the results of our investigation, the NO₂⁻ levels decreased in a dose-dependent manner, which indicated the effects of senescence. We also measured the serum NO₂⁻ levels in AMA and control mice before pregnancy, at E14.5, and at E18.5. Consistent with previous in vitro results, the serum NO₂⁻ levels in AMA mice at the E18.5 period were significantly lower than those in control mice during the same period (Supplementary Figure 7). These results supported the fact that human AMA and the AMA mouse model exhibited increasing blood pressure despite lower levels of sFlt-1. Unfortunately, we could not discover evidence that NO₂⁻ was decreased in aged HDP patients. Moreover, the limitation of this study includes the limited number of human serum samples. Accordingly, further investigation and the collection of more samples will be needed.

In summary, we established an AMA mouse model using aged pregnant ICR mice and discovered several novel findings. The AMA mouse model had similarities to the complication phenotypes of human AMA. The AMA mouse model demonstrated HDP as blood pressure increased in late gestation and decreased soon after delivery. Both human AMA and the AMA mouse model demonstrated HDP and lower serum levels of sFlt-1 than young subjects. Our mouse model showed similar characteristics to those of human aged HDP patients.

This is the first report that AMA mice and human aged HDP patients manifested lower serum levels of sFlt-1 despite complicating hypertension. In previous studies, the serum sFlt-1 level in HDP patients has not been categorized according to age. Our results demonstrated that the serum sFlt-1 level in aged HDP patients is lower than that in the control group. These results indicated that the serum levels of sFlt-1, as a marker of HDP, should be evaluated depending on maternal age.

Additional studies will be needed to verify the mechanism of hypertension with low serum sFlt-1. For future investigations, we suggest that the recruitment of clinical subjects and analysis of human AMA blood vessels will be needed.

Summary from the corresponding author

HDP is one of the major complications that arises during pregnancy, particularly in AMA. However, there has been limited information derived from basic research regarding the relationship between HDP and AMA. In our research, aged pregnant ICR mice exhibited the same characteristics as human AMA. Obesity, declining fertility, small for gestational age (SGA), IUFD, elevated blood pressure, and placental dysfunction are complications in AMA. AMA mice and human AMA patients exhibited lower serum sFlt-1 levels than control subjects. Our findings provide evidence that HDP occurred concurrently with lower serum sFlt-1 levels compared with younger groups, and these findings will contribute to the future management of HDP in AMA.

Acknowledgements We thank the Department of Molecular and Cell Biology, Graduate School of Agricultural Science, Tohoku University for the financial support. This research was also supported by grants from the Grants-in-Aid for Scientific Research and the Takeda Science Foundation. This study was supported by the Center for Medical Research and Education, Graduate School of Medicine, Osaka University. We thank Ms. Haruyo Sakamoto for her excellent technical support in this investigation. Finally, we appreciate Dr. Stephen Gadd's very helpful English editing.

Compliance with ethical standards

Conflict of interest The authors declare that they have no conflict of interest.

References

- Favilli A, Pericoli S, Acanfora MM, Bini V, Di Renzo GC, Gerli S. Pregnancy outcome in women aged 40 years or more. *J Matern Fetal Neonatal Med.* 2012;25:1260–3.
- Yogev Y, Melamed N, Bardin R, Tenenbaum-Gavish K, Ben-Shitrit G, Ben-Haroush A. Pregnancy outcome at extremely advanced maternal age. *Am J Obstet Gynecol.* 2010;203:558.e551–7.
- Wang Y, Tanbo T, Abyholm T, Henriksen T. The impact of advanced maternal age and parity on obstetric and perinatal outcomes in singleton gestations. *Arch Gynecol Obstet.* 2011;284:31–7.
- Luke B, Brown MB. Elevated risks of pregnancy complications and adverse outcomes with increasing maternal age. *Hum Reprod.* 2007;22:1264–72.
- Reddy UM, Ko CW, Willinger M. Maternal age and the risk of stillbirth throughout pregnancy in the United States. *Am J Obstet Gynecol.* 2006;195:764–70.
- Mutz-Dehbalae I, Scheier M, Jerabek-Klestil S, Brantner C, Windbichler GH, Leitner H, et al. Perinatal mortality and advanced maternal age. *Gynecol Obstet Invest.* 2014;77:50–7.
- Salihu HM, Wilson RE, Alio AP, Kirby RS. Advanced maternal age and risk of antepartum and intrapartum stillbirth. *J Obstet Gynaecol Res.* 2008;34:843–50.
- Kumasawa K, Ikawa M, Kidoya H, Hasuwa H, Saito-Fujita T, Morioka Y, et al. Pravastatin induces placental growth factor (PGF) and ameliorates preeclampsia in a mouse model. *Proc Natl Acad Sci USA.* 2011;108:1451–5.
- Intapad S, Warrington JP, Spradley FT, Palei AC, Drummond HA, Ryan MJ, et al. Reduced uterine perfusion pressure induces hypertension in the pregnant mouse. *Am J Physiol Regul Integr Comp Physiol.* 2014;307:R1353–7.
- Iriyama T, Wang W, Parchim NF, Song A, Blackwell SC, Sibai BM, et al. Hypoxia-independent upregulation of placental hypoxia inducible factor-1 α gene expression contributes to the pathogenesis of preeclampsia. *Hypertension.* 2015;65:1307–15.
- Podjarny E, Losonczy G, Baylis C. Animal models of preeclampsia. *Semin Nephrol.* 2004;24:596–606.
- Nguyen TM, Nakamura H, Wakabayashi A, Kanagawa T, Koyama S, Tsutsui T, et al. Estimation of mouse fetal weight by ultrasonography: application from clinic to laboratory. *Lab Anim.* 2012;46:225–30.
- Toutouna L, Nikolakopoulou P, Poser SW, Masjkur J, Arps-Forker C, Troullinaki M, et al. Hes3 expression in the adult mouse brain is regulated during demyelination and remyelination. *Brain Res.* 2016;1642:124–30.
- Matsusaka H, Ide T, Matsushima S, Ikeuchi M, Kubota T, Sunagawa K, et al. Targeted deletion of p53 prevents cardiac rupture after myocardial infarction in mice. *Cardiovasc Res.* 2006;70:457–65.
- La Perle KM, Jhiang SM, Capen CC. Loss of p53 promotes anaplasia and local invasion in ret/PTC1-induced thyroid carcinomas. *Am J Pathol.* 2000;157:671–7.
- Seah C, Levy MA, Jiang Y, Mokhtarzada S, Higgs DR, Gibbons RJ, et al. Neuronal death resulting from targeted disruption of the Snf2 protein ATRX is mediated by p53. *J Neurosci.* 2008;28:12570–80.
- Kusminski CM, Park J, Scherer PE. MitoNEET-mediated effects on browning of white adipose tissue. *Nat Commun.* 2014;5:3962.
- Bladier C, Wolvetang EJ, Hutchinson P, de Haan JB, Kola I. Response of a primary human fibroblast cell line to H₂O₂: senescence-like growth arrest or apoptosis? *Cell Growth Differ.* 1997;8:589–98.
- Frippiat C, Chen QM, Remacle J, Toussaint O. Cell cycle regulation in H(2)O(2)-induced premature senescence of human diploid fibroblasts and regulatory control exerted by the papilloma virus E6 and E7 proteins. *Exp Gerontol.* 2000;35:733–45.
- Phipps SM, Berletch JB, Andrews LG, Tollefsbol TO. Aging cell culture: methods and observations. *Methods Mol Biol.* 2007;371:9–19.
- Zhou X, Zhang GY, Wang J, Lu SL, Cao J, Sun LZ. A novel bridge between oxidative stress and immunity: the interaction between hydrogen peroxide and human leukocyte antigen G in placental trophoblasts during preeclampsia. *Am J Obstet Gynecol.* 2012;206:447.
- Chen H, Li Y, Tollefsbol TO. Cell senescence culturing methods. *Methods Mol Biol.* 2013;1048:1–10.
- Umesawa M, Kobashi G. Epidemiology of hypertensive disorders in pregnancy: prevalence, risk factors, predictors and prognosis. *Hypertens Res.* 2017;40:213–20.
- Zeisler H, Llorba E, Chantraine F, Vatish M, Staff AC, Sennstrom M, et al. Predictive value of the sFlt-1:PIGF ratio in women with suspected preeclampsia. *N Engl J Med.* 2016;374:13–22.
- Puttakitpong P, Phupong V. Combination of serum angiopoietin-2 and uterine artery Doppler for prediction of preeclampsia. *Hypertens Res.* 2016;39:95–99.

26. Luke B, Brown MB. Contemporary risks of maternal morbidity and adverse outcomes with increasing maternal age and plurality. *Fertil Steril*. 2007;88:283–93.
27. Sakakibara Y, Hashimoto S, Nakaoka Y, Kouznetsova A, Hoog C, Kitajima TS. Bivalent separation into univalents precedes age-related meiosis I errors in oocytes. *Nat Commun*. 2015;6:7550.
28. Kazushi Watanabe KN, Tanaka Kanji, Metoki Hirohito, Suzuki Yoshikatsu. Statement of the society: outline of definition and classification of “Pregnancy induced Hypertension (PIH)”. *Hypertens Res Pregnancy*. 2013;1:3–4.
29. Hypertension in Pregnancy. Report of the American College of Obstetricians and Gynecologists’ task force on hypertension in pregnancy. *Obstet Gynecol*. 2013;122:1122–31.
30. Ohkuchi A, Hirashima C, Takahashi K, Suzuki H, Matsubara S. Prediction and prevention of hypertensive disorders of pregnancy. *Hypertens Res*. 2017;40:5–14.
31. Makris A, Yeung K, Farrell P, Heffernan S, Thompson J, Xu B, et al. OS061. Placental growth factor reduces blood pressure and proteinuria in experimental preeclampsia. *Pregnancy Hypertens*. 2012;2:210.
32. Alexander BT, Kassab SE, Miller MT, Abram SR, Reckelhoff JF, Bennett WA, et al. Reduced uterine perfusion pressure during pregnancy in the rat is associated with increases in arterial pressure and changes in renal nitric oxide. *Hypertension*. 2001;37:1191–5.
33. Matsubara K, Matsubara Y, Mori M, Uchikura Y, Hamada K, Fujioka T, et al. Immune activation during the implantation phase causes preeclampsia-like symptoms via the CD40-CD40 ligand pathway in pregnant mice. *Hypertens Res*. 2016;39:407–14.
34. Maynard SE, Min JY, Merchan J, Lim KH, Li J, Mondal S, et al. Excess placental soluble fms-like tyrosine kinase 1 (sFlt1) may contribute to endothelial dysfunction, hypertension, and proteinuria in preeclampsia. *J Clin Invest*. 2003;111:649–58.
35. Levine RJ, Maynard SE, Qian C, Lim KH, England LJ, Yu KF, et al. Circulating angiogenic factors and the risk of preeclampsia. *N Engl J Med*. 2004;350:672–83.
36. Maynard SE, Venkatesha S, Thadhani R, Karumanchi SA. Soluble Fms-like tyrosine kinase 1 and endothelial dysfunction in the pathogenesis of preeclampsia. *Pediatr Res*. 2005;57:1r–7r.
37. Tomimatsu T, Mimura K, Endo M, Kumasawa K, Kimura T. Pathophysiology of preeclampsia: an angiogenic imbalance and long-lasting systemic vascular dysfunction. *Hypertens Res*. 2017;40:305–10.
38. Moore Simas TA, Crawford SL, Solitro MJ, Frost SC, Meyer BA, Maynard SE. Angiogenic factors for the prediction of preeclampsia in high-risk women. *Am J Obstet Gynecol*. 2007;197:244.e241–8.
39. Staff AC, Braekke K, Harsem NK, Lyberg T, Holthe MR. Circulating concentrations of sFlt1 (soluble fms-like tyrosine kinase 1) in fetal and maternal serum during pre-eclampsia. *Eur J Obstet Gynecol Reprod Biol*. 2005;122:33–39.
40. Rudolph KL, Chang S, Lee HW, Blasco M, Gottlieb GJ, Greider C, et al. Longevity, stress response, and cancer in aging telomerase-deficient mice. *Cell*. 1999;96:701–12.
41. Tyner SD, Venkatachalam S, Choi J, Jones S, Ghebranious N, Igelmann H, et al. p53 mutant mice that display early ageing-associated phenotypes. *Nature*. 2002;415:45–53.
42. Varela I, Cadinanos J, Pendas AM, Gutierrez-Fernandez A, Folgueras AR, Sanchez LM, et al. Accelerated ageing in mice deficient in Zmpste24 protease is linked to p53 signalling activation. *Nature*. 2005;437:564–8.
43. Minamino T. Endothelial cell senescence in human atherosclerosis: role of telomere in endothelial dysfunction. *Circulation*. 2002;105:1541–4.
44. Chang E, Harley CB. Telomere length and replicative aging in human vascular tissues. *Proc Natl Acad Sci USA*. 1995;92:11190–4.
45. Kunieda T, Minamino T, Nishi J, Tateno K, Oyama T, Katsuno T, et al. Angiotensin II induces premature senescence of vascular smooth muscle cells and accelerates the development of atherosclerosis via a p21-dependent pathway. *Circulation*. 2006;114:953–60.
46. Miyachi H, Minamino T, Tateno K, Kunieda T, Toko H, Komuro I. Akt negatively regulates the in vitro lifespan of human endothelial cells via a p53/p21-dependent pathway. *EMBO J*. 2004;23:212–20.
47. Rosso A, Balsamo A, Gambino R, Dentelli P, Falcioni R, Cas-sader M, et al. p53 Mediates the accelerated onset of senescence of endothelial progenitor cells in diabetes. *J Biol Chem*. 2006;281:4339–47.
48. Cross CE, Tolba MF, Rondelli CM, Xu M, Abdel-Rahman SZ. Oxidative stress alters miRNA and gene expression profiles in villous first trimester trophoblasts. *Biomed Res Int*. 2015;2015:257090.
49. Zdanov S, Remacle J, Toussaint O. Establishment of H₂O₂-induced premature senescence in human fibroblasts concomitant with increased cellular production of H₂O₂. *Ann N Y Acad Sci*. 2006;1067:210–6.